UC Irvine

Title

Using neutral beams as a light ion beam probe (invited)a)

Permalink

https://escholarship.org/uc/item/56g6n67x

Journal

Review of Scientific Instruments, 85(11)

ISSN

0034-6748

Authors

Chen, Xi
Heidbrink, WW
Van Zeeland, MA
et al.

Publication Date

2014-11-01

DOI

10.1063/1.4889733

Peer reviewed

CrossMark
click for updates

Using neutral beams as a light ion beam probe (invited)[a]

Xi Chen,[1,b] W. W. Heidbrink,[2] M. A. Van Zeeland,[3] G. J. Kramer,[4] D. C. Pace,[3] C. C. Petty,[3] M. E. Austin,[5] R. K. Fisher,[3] J. M. Hanson,[6] R. Nazikian,[4] and L. Zeng[7]

[1]*Oak Ridge Institute for Science and Education, Oak Ridge, Tennessee 37831, USA*
[2]*University of California Irvine, Irvine, California 92697, USA*
[3]*General Atomics, P.O. Box 85608, San Diego, California 92186-5608, USA*
[4]*Princeton Plasma Physics Laboratory, P.O. Box 451, Princeton, New Jersey 08543, USA*
[5]*University of Texas at Austin, Austin, Texas 78712, USA*
[6]*Columbia University, New York, New York 10027, USA*
[7]*University of California Los Angeles, Los Angeles, California 90095, USA*

By arranging the particle first banana orbits to pass near a distant detector, the light ion beam probe (LIBP) utilizes orbital deflection to probe internal fields and field fluctuations. The LIBP technique takes advantage of (1) the *in situ*, known source of fast ions created by beam-injected neutral particles that naturally ionize near the plasma edge and (2) various commonly available diagnostics as its detector. These born trapped particles can traverse the plasma core on their inner banana leg before returning to the plasma edge. Orbital displacements (the forces on fast ions) caused by internal instabilities or edge perturbing fields appear as modulated signal at an edge detector. Adjustments in the q-profile and plasma shape that determine the first orbit, as well as the relative position of the source and detector, enable studies under a wide variety of plasma conditions. This diagnostic technique can be used to probe the impact on fast ions of various instabilities, e.g., Alfvén eigenmodes (AEs) and neoclassical tearing modes, and of externally imposed 3D fields, e.g., magnetic perturbations. To date, displacements by AEs and by externally applied resonant magnetic perturbation fields have been measured using a fast ion loss detector. Comparisons with simulations are shown. In addition, nonlinear interactions between fast ions and independent AE waves are revealed by this technique. © 2014 AIP Publishing LLC. [http://dx.doi.org/10.1063/1.4889733]

I. INTRODUCTION

To achieve the very high temperature required for fusion reaction in a magnetically confined plasma, additional plasma heating is usually necessary. Neutral beam injection (NBI) is one of the most widespread heating techniques in existing devices and will be employed in ITER. Injected neutrals ionize in charge-exchange and electron-impact-ionization collisions, becoming fast ions in the process. The fast ions heat the plasma through Coulomb collisions with the background electrons and ions. In this paper, we present a novel and innovative diagnostic approach—light ion beam probe (LIBP), which utilizes some of the beam ions as test particles.

Internal magnetic field measurements, including field fluctuations are important for studies of instabilities, transport, and 3D fields effects. There are some existing techniques, such as polarimetry, but the measurements are challenging. Here, we introduce the light ion beam probe technique as a simple and relatively economical method. By pairing with various different available diagnostics as its detector, beam-ion orbital displacements due to internal or externally applied fields or field fluctuations result in modulations in the detected signal.

In this paper, the published physics results that inspired the LIBP technique are briefly reviewed and new experiments specially designed for the LIBP are presented. Emphasis is given to the diagnostic setup and possible applications. The principle of the light ion beam probe is described in Sec. II. Examples using fast ion loss diagnostics as LIBP detector to study externally applied magnetic perturbations (MPs)[1] for edge localized mode (ELM)[2] suppression and Alfvén eigenmodes (AEs)[3] are given in Sec. III. A few applications using other diagnostics as LIBP detector are mentioned in Sec. IV where the limitation and the potential implementation of the LIBP are also discussed.

II. PRINCIPLE OF LIBP

One advantage of the LIBP is it uses an *in situ*, known source of fast ions created by the neutral beam injection. There are always some naturally born beam ions near the plasma edge and in the scrape-off layer (SOL). Usually, not much attention is paid to those particles because they are only a very small fraction of the total beam ions and loss of these particles does not cause appreciable power loss. Here, we use these edge fast ions as test particles. The LIBP uses the orbital deflection to make measurements analogous to how a heavy ion beam probe[4,5] measures the electric fields. The neutral beam ions (deuterium) are much lighter than the ones used by HIBP (sodium, potassium, cesium, etc.), therefore we call the technique a "light ion beam probe".

Another advantage of the LIBP is it uses various available diagnostics as its detector, such as particle diagnostics (e.g., fast ion loss detector), charge exchange spectrometers (e.g., fast ion Dα diagnostic), imaging diagnostics (e.g., infrared camera). In this paper, the LIBP technique and applications are presented primarily using the fast ion loss detector for detection. Fast ion loss detection has been used to measure loss of super-thermal particles (α-particles or fast ions) for a long time: from the Faraday cups on the tokamak of Fontenay-aux-Roses (TFR), to the silicon surface barrier detector on the Princeton Large Torus (PLT),[6,7] to the scintillator based detector on the Tokamak Fusion Test Reactor (TFTR).[8] Now many devices are equipped with various forms of fast ion loss detectors with different names (e.g., FILD, FIL, SLIP, SP, sFILP, etc.).[9–16] ("FILD" will be used in the rest of the paper.) A common fast ion loss detector is a scintillator-based detector with a charge-coupled device (CCD) camera and/or photomultiplier (PMT) detection system. The FILD works as a magnetic spectrometer and detects fast particles that reach its location on the machine outer wall. Fast particles, gyrating into the probe through a collimating aperture, impinge upon the scintillator and induce light. Particles with different gyroradii and pitch angle (relative to magnetic field direction) will encounter different positions on the scintillator plate. The scintillator emission pattern presents the energy and pitch of the lost particles while the emission intensity carries information of the mode frequency, amplitude, etc.

The HIBP utilizes the first gyro-orbit, while the LIBP uses the first poloidal orbit. Particle orbits generally fall into two classes: passing and trapped. LIBP uses a particular kind of trapped (or banana) orbits, which start from the far edge or the SOL of the plasma and closely approach the edge detector on the first poloidal transit. The trapped orbit width is inversely proportional to the plasma current. At low plasma current, the banana orbit can be wide enough that the inner leg of the banana orbit passes through the plasma interior, allowing it to probe the internal fields or modes. Because these fast ions traverse the perturbation quickly and only once, the imprint of the wave-particle interactions is preserved when these test particles exit the plasma.

A typical LIBP setup along with an unperturbed fast ion orbit on a toroidal device is illustrated in Fig. 1. The unperturbed orbit starts near the far edge of the plasma and closely approaches the FILD after one poloidal bounce in the quiescent plasma equilibrium. Different neutral beam system can be connected to the FILD by changing the magnetic equilibrium, principally the particle phase, the particle is pushed radially outwards and strikes the FILD while, at other phases, the particle misses the FILD (e.g., is pushed radially inwards). The orbital deflection results in a modulation of the FILD signal at the frequency of the perturbing field. By tracking both in time and in frequency, coherent loss induced by the individual mode can be extracted from the FILD signal.

When the perturbing field becomes stronger, the force on the fast ion is stronger and the orbital deflection is larger. The consequence of the larger orbital deflection is that particles born *further inside* the plasma are able to reach the FILD. Because of the steep gradient of the ionization profile near the plasma edge and in the SOL, there are *more* fast ions born *further inside*. This leads to higher fast ion flux at the FILD when the perturbing field is stronger. It has been observed in the experiments on the DIII-D tokamak that the coherent fast-ion flux at the FILD scales linearly with the mode amplitude. The orbital deflection or the force on the fast ion imparted by an individual mode (or perturbing field) can be quantified by the radial displacement (ζ), which can be experimentally inferred using the model

$$\zeta \approx (\Delta F / \bar{F}) L_i, \tag{1}$$

where ΔF is the coherent fast-ion flux at the FILD, $\bar{F}$ is the unperturbed fast-ion flux at the FILD, and L_i is the ionization scale length at the point where the unperturbed orbits start. L_i can be derived from the calculated edge beam deposition profile, which depends on geometry, T_e, and the effective ion charge (Z_{eff}) as well as the density. The linear dependence on n_e is much stronger than on T_e or Z_{eff}, so the density scale length L_n can be used instead of L_i in Eq. (1) ($L_n \sim L_i$ near the edge). The details of the model such as the calculation of each term in the formula, the assumptions and approximations applied, and the limitations are given in Ref. 17. Note that in order to infer the radial displacement using the model [Eq. (1)], measurements with LIBP-beam turned off are needed for the calculations of the "DC" loss $\bar{F}$ and modulated perturbations that lead to "AC" (coherent) loss ΔF.

Modulations in the FILD signal induced by Alfvén waves with $\delta B_{peak}/B \leq 1 \times 10^{-3}$ have been observed on DIII–D. The LIBP can be applied to study fluctuating magnetic fields or
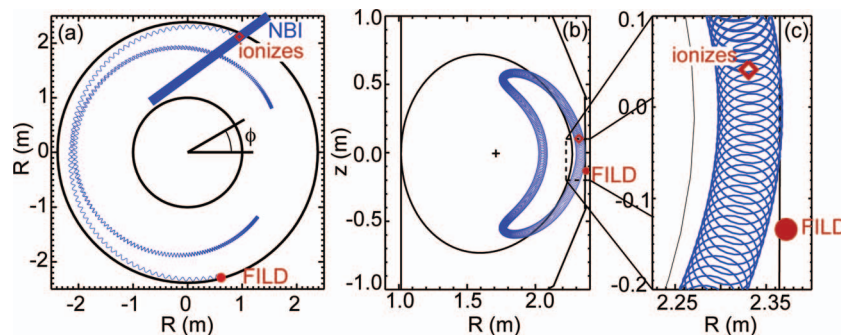

FIG. 1. A typical unperturbed beam-ion orbit (blue) that LIBP uses in (a) top view, (b) elevation, (c) close-up: a beam ion (red diamond) born in the far edge or SOL and approaches the FILD (red dot) on the first poloidal bounce. When there is a perturbing field, at certain wave-phase, the particle can be pushed outwards and lost to the FILD.

changes in the equilibrium magnetic field at this magnitude, as the examples given in Sec. III demonstrate.

III. EXAMPLES OF IMPLEMENTATION OF LIBP

A. Effects of applied 3D magnetic perturbations on fast ion loss

Non-axisymmetric (or 3D) fields can come from an imperfect magnetic configuration such as the error field or toroidal field (TF) ripple as well as intentional externally applied 3D magnetic perturbation such as those used to suppress ELMs. Fast particles, due to their relatively long confined path lengths and low collisionality, are particularly sensitive to the non-axisymmetric fields. In fact, simulations show that ELM mitigation coils (referred to as ELM-coil in this paper) can induce up to 5% loss of beam ions in ITER.[18]

The LIBP technique has been used to investigate the effects of applied 3D fields on DIII-D.[19] The experiments are carried out in MHD-quiescent L-mode plasmas with externally applied n = 2 field from ELM-coils. A counter-NBI (with respect to the plasma current direction) and a co-NBI are utilized as the LIBP source beam successively. Lost ion detection is accomplished using two spatially separated detectors that are separated toroidally by 60° and poloidally by ~45°. Different spatial locations and slightly different detection ranges (in pitch and energy space) of the two detectors allow the detection of orbits from a wider range of configuration and velocity space. A 25 Hz travelling waveform is applied to the ELM-coils, therefore, the perturbations rotate past both the beams and the FILDs. The fast-ion fluxes at both FILDs clearly exhibit a modulation at the ELM-coil frequency. (Signal from only one of the two FILDs is shown in Fig. 2.) The prompt loss feature can be seen in the close-up plot, the loss signal appears <20 μs (within one poloidal transit time ~40 μs) after the source beam switch-on and disappears rapidly after the beam turn-off. Data from the time windows near the beginning (t ~ 1050 ms) and near the end (t ~ 2000 ms) of the co-current beam injection are applied to calculate the radial displacement of fast ions induced by the n = 2 fields. These two time windows were chosen because $\bar{F}$ can be estimated using the data right before and immediately after the beam injection. Since the perturbing field is the same in the two time windows, the radial displacements should not change. The experimentally inferred radial displacement $\zeta \approx (\Delta F/\bar{F})L_n$ at both time windows is ~3 cm with an uncertainty of ~1.7 cm. The simulations, presented in Ref. 19 using a FORTRAN based full-orbit solver with M3D-C1[20] calculated perturbed kinetic profiles and fields, successfully reproduce the phase of the modulated loss signal with respect to the ELM-coil currents but show a slightly smaller radial displacement of ~1 cm. (The radial displacement in the simulation is defined as the radial difference between the perturbed and unperturbed orbits at the midplane.) The small discrepancy between the experimental radial displacement and the lower simulated ($\Delta F/\bar{F}$) could be due to the fact that in the simulation, the particle is considered as lost at the FILD if it is within 5 cm to the FILD location which can lead to a slight underestimation of the radial displacement. The neglect of a
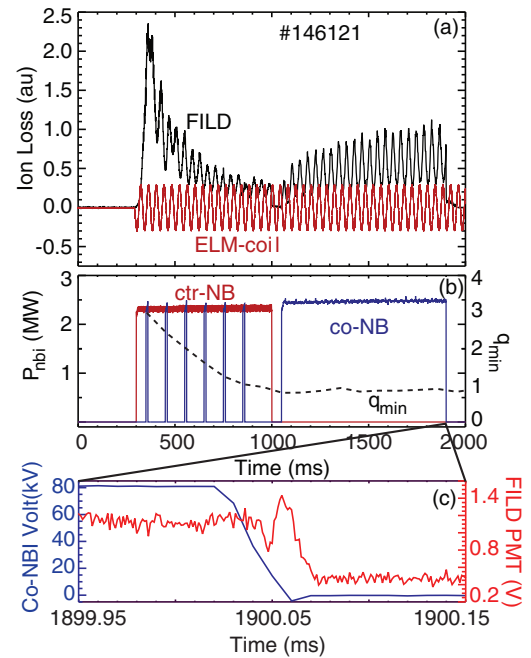

FIG. 2. (a) The fast ion flux at the FILD (black) is modulated at the rotating frequency of the n = 2 field (red) from the ELM-coils. (b) A counter-current NBI (red) is utilized as LIBP source beam (a few co-current NBI blips are injected for diagnostics) and later in time, a co-current NBI (blue) is utilized as LIBP source beam. The overall FILD loss signal tracks the plasma q-profile evolution (q_{min} is shown) due to its prompt loss nature, which can also be seen by comparing (c) the NBI time trace (blue) and the loss signal (red) near t = 1900 ms. The loss signal disappears within one poloidal transit time after the beam is switched off.

significant n = 4 component in the applied simulation fields and the equilibrium electric field can be another cause.

New experiments with edge density perturbations using a small deuterium gas puff have been conducted to test the model [Eq. (1)]. Similar to the experiments in Ref. 19, a 25 Hz rotating n = 1 field from ELM-coils is applied in L-mode plasmas during the plasma current flat top with steady LIBP beam injection. In these experiments, the FILD signal clearly shows a coherent 25 Hz modulation (Fig. 3) similar to previous observations in Ref. 19. Several 10 ms-duration pulses of deuterium gas are puffed into the vessel. The puff amount is adjusted so that the plasma density is unaffected except near the edge and in the SOL (Fig. 3) where the majority of the FILD detected fast ions are born. The response of FILD signal to the small gas puff qualitatively agrees with the model: the signal increases with the increased ionization (thus, the ion source). A quantitative test of the model [Eq. (1)] appears in Sec. III B.

B. Radial displacement of fast ions due to individual Alfvén eigenmodes

Energetic particles are important for plasma heating and current drive while they can also drive instabilities such as Alfvén eigenmodes. AEs can cause redistribution and loss of the energetic particles. AE-induced fast ion losses have been measured on many devices and in various plasmas but these are usually lost after completing many circuits around the
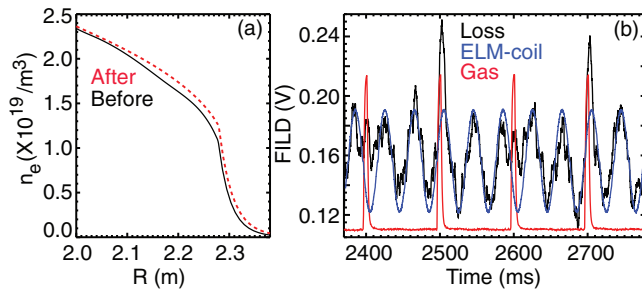
FIG. 3. Small amount deuterium gas is puffed into the plasma every 100 ms. (a) Each gas puff results in a small increase in the edge plasma density (black solid line-before; red dashed line-after). The edge ionization is proportional to the density; therefore, there is a small increase in the edge ionization after each gas puff. (b) The FILD loss (black) is modulated at the rotating frequency (25 Hz) of $n = 1$ field (blue) from the ELM-coils. On top of the modulation by the ELM-coil fields, loss at FILD increases each time when there is gas (red) puffed independent of the ELM-coil field phase.

FIG. 5. Radial displacements (ζ) for $n = 2$ RSAE between 325 and 330 ms in discharge 146096 is experimentally determined (color contour) at a range of mode amplitudes (using ECE electron temperature fluctuation measurements as a measure of the mode amplitude). Typical error is shown.

torus. Therefore, some of the details of the wave-particle interactions, e.g., the radial displacement (the force on the fast ion) due to individual modes, cannot be quantitatively determined whereas it is made possible through the LIBP technique using the first poloidal bounce.

An example (first reported in Ref. 21) is shown in Fig. 4, during the early plasma current ramping phase in a neutral beam heated reversed magnetic shear plasma, two tangential co-current neutral beams are alternatively injected. The 30 L beam is the LIBP source beam and the midplane FILD is the LIBP detector. Coherent losses induced by TAEs (with nearly constant frequencies) and RSAEs (with sweeping-up frequencies) are detected. The prompt loss fea-
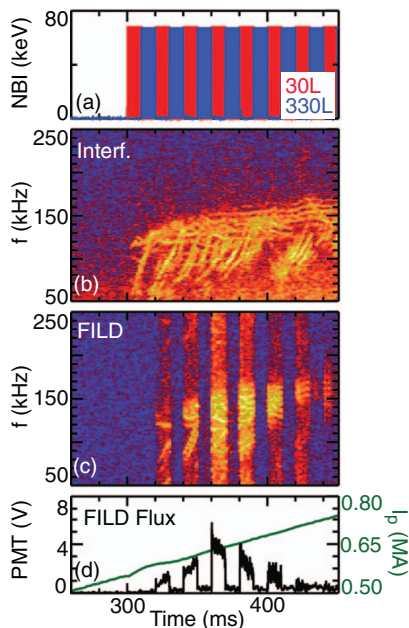

FIG. 4. In a reversed magnetic shear plasma 146096: (a) Two co-current NBIs 30 L (red) and 330 L (blue) alternatively inject and (b) a lot AEs are driven unstable as can be seen from the line-integrated density fluctuations measured by the interferometer. (c) FILD detects coherent loss from 30 L beam only and (d) the total fast ion flux at FILD (black) evolution tracks the plasma current (green).
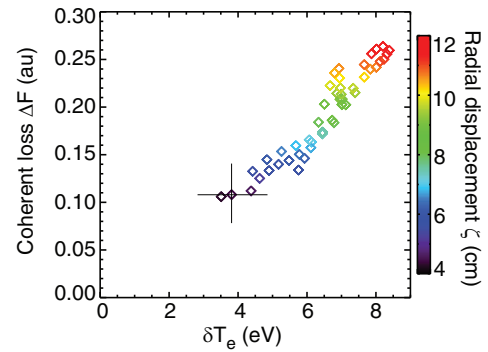
ture is reflected in the toroidal dependence of FILD signal, that is, the fast-ion flux at the FILD only comes from the 30 L beam, which is identical to the 330 L beam except for its toroidal location. As in the example shown in Fig. 2, by comparing to the source neutral beam timing, the prompt mechanism is also confirmed by the fast (within one poloidal transit period) rising and decaying of the escaping fast-ion flux. Direct measurements of the radial displacement due to individual modes are achieved as demonstrated in Fig. 5. In this case, it has been found that the single $n = 2$ RSAE at an amplitude of ($\delta T_e \sim 7$ eV, equivalent to $\delta B/B \sim 0.1\%$) can cause an as large as 10 cm radial displacement of a fast ion (for reference, the gyroradius is about 4–5 cm).

As mentioned in Sec. III A, the quantitative validation of the model for the radial displacement calculation is achieved in carefully designed experiments for AE study with LIBP using gas puffing. The duration, amount, and timing of the gas puff are adjusted to meet the following three criteria: (1) the perturbation is small enough so that the plasma equilibrium and the AE modes are not affected; (2) the perturbation is large enough so that changes can be seen in the plasma edge electron density (thus, the beam ionization); and (3) the perturbation takes place in the middle of a period that the modes (especially the selected one) have relatively steady amplitudes. Since the radial displacement ζ due to a given mode is expected to remain the same since the mode is not altered by the gas puffing, the coherent loss ΔF, the "DC" loss $\bar{F}$, and the edge density scale length L_n ($\approx L_i$) should all change following the gas puff such that $\zeta \approx (\Delta F/\bar{F})L_n$ remains essentially unchanged. As illustrated in Fig. 6, coherent loss caused by TAEs and RSAEs are detected at the FILD from 500 to 540 ms when the LIBP source beam is switched on. Within this time window, a 10 ms deuterium gas is puffed into the vessel at t = 520 ms. The modes stay the same after the gas puff but changes in fast-ion flux (brighter in color) can be seen in the spectrogram of the FILD signal. A 95 kHz TAE is traced to quantitatively test the model. The values of relevant quantities before (t $\sim$ 515 ms) and after (t $\sim$ 525 ms) the gas puff are listed in Table I. The radial displacement by this TAE is the same for both times, which quantitatively validates the model.
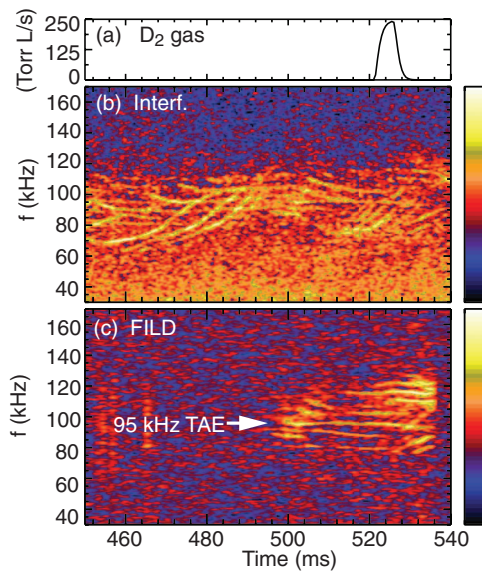
FIG. 6. (a) Small amount deuterium gas is puffed into the plasma. (b) The mode spectrum is not affected by the gas puffing as that can be seen from the interferometer data. However, (c) the loss at the FILD is affected. A 95 kHz TAE is tracked in order to quantitatively test the radial displacement model [Eq. (1)].

C. Nonlinear fast ion losses induced by independent Alfvén waves

Although it is well known that multiple modes cause larger fast-ion transport than a single mode, the underlying physics is not always clear or well tested. Significant experimental effort has been made on measuring fast ion losses in the presence of many classes of instabilities in many different devices. A clear detection of one kind of nonlinear multi-wave-particle interactions is achieved through LIBP measurement—the nonlinear fast ion loss induced by independent AEs on DIII-D (first reported in Ref. 22). As shown in Figs. 7(b) and 7(c), coherent loss due to two RSAEs and two TAEs are detected at the FILD. Interestingly, losses at the sum and second harmonic frequencies of the RSAEs and TAEs are also observed. More interestingly, these additional nonlinear oscillations are only observed in the fast-ion flux, not in other plasma fluctuation measurements (e.g., δB, δT_e [Fig. 7(a)], δn_e, etc.). The prompt mechanism is again confirmed through the toroidal beam source dependence and the fast time response to the beam switch on/off. The nonlinearity in the fast-ion loss signal and its absence in other plasma wave measurements are confirmed through bi-coherence analyses. As demonstrated in Ref. 22, this nonlinear loss results from the particle orbital response to independent waves instead of the conventional wave-wave beating. While the nonlinear multi-mode fast-ion interaction likely occurs on DIII-D
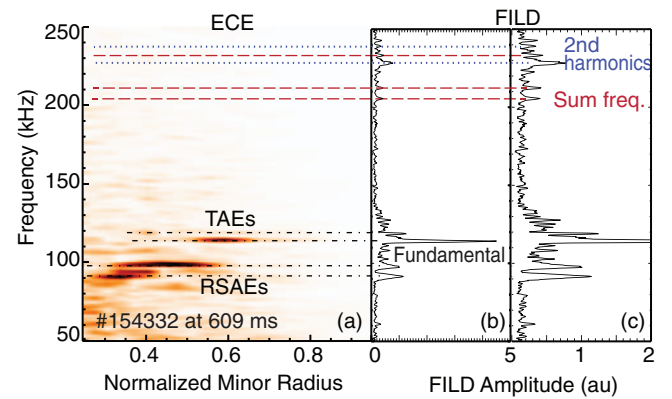

FIG. 7. In discharge 154332, (a) there are two RSAEs (91.7 and 98.2 kHz) and two TAEs (114.2 and 119.4 kHz) detected by ECE (Mode frequencies are quoted at t = 609 ms). (b) FILD detects coherent losses from these four modes at not only the fundamental frequencies (indicated by black dotted-dashed lines) but also the sum (205.9, 211.1, and 233.6 kHz, indicated by red dashed lines) and 2nd harmonic frequencies of these modes (228.4 and 238.8 kHz, indicated by blue dotted lines). (c) For better visualization of the peaks with lower amplitudes in the FILD spectra, it is plotted in reduced loss amplitude range.

and other devices when two or more modes are interacting with energetic particles, the information is for the first time preserved and able to be unfolded through LIBP measurements.

The data provide a stringent test for theoretical models and numerical codes. Full orbit SPIRAL[23] simulations including NOVA[24] calculated AE structures with experimental mode amplitudes, slowing-down and pitch-angle scattering effects, beam ionization profile (including that in the SOL), and realistic machine wall models, qualitatively reproduce the nonlinear loss measurements.

IV. SUMMARY AND DISCUSSION

The light ion beam probe is an economical method to probe internal fields: it utilizes the standard heating and fueling neutral beam as a particle source and commonly available fast ion instruments as detector. LIBP is a simple technique: it utilizes the first poloidal orbit of beam ions. The first orbit, connecting a given FILD and neutral beam located at different toroidal locations, can pass through different regions of the plasma. In addition, different initial pitch angles can be obtained from different beam injection geometries (e.g., tangential vs perpendicular injection) and different FILDs might provide different detection ranges. By selecting the LIBP source beam and detector strategically, adjusting plasma current, plasma shape (e.g., gap between the last closed flux surface and the vessel wall), edge density, etc., a large radial extent can be accessed by LIBP.

Various MHD instabilities, such as AE and NTM, and non-axisymmetric fields, such as TBM and ELM coil fields, along with plasma response to these externally applied fields can be studied using the LIBP. LIBP measurements for plasma response in H-mode plasmas on DIII-D have been obtained. Despite the complication by the ELMs, preliminary analysis indicates some difference in the fast ion flux at different plasma response regimes and it is consistent with theoretical predictions.

TABLE I. Radial displacement calculations before and after gas puff for shot 154334.

Gas	ΔF	$\bar{F}$	Ln (m)	δTe (eV)	ζ (cm)
Before	0.06 ± 0.01	0.42 ± 0.04	0.38 ± 0.1	2.5 ± 1	5.4 ± 1.7
After	0.07 ± 0.01	0.52 ± 0.04	0.43 ± 0.1	2.3 ± 1	5.8 ± 1.7

As demonstrated by the few examples in this paper, LIBP measurements provide unique opportunities for quantitatively testing and comparison of theoretical models and numerical codes. However, several issues limit more accurate code validation. The uncertainties in experimental measurements of the edge density or the ionization profile introduce uncertainty in the calculated radial displacements. Due to the finite-size and central (near beamline axis) peaked profile of the neutral beam, the orbit displacement in directions other than the radial direction might be important for some situations. To reduce this effect, the unperturbed orbit should be selected to pass through the center of the beamline cross section. A "pencil beam" (small diameter diagnostic beam) will be optimal. Furthermore, the model for radial displacement calculations is only applicable for the linear region on the edge ionization profile. That is, if the mode is strong enough to eject fast ions far from the region where the unperturbed orbits start, the variation in the ionization scale length maybe large enough that the radial displacement cannot be obtained using this simple model anymore. The equilibrium electric field has a negligible effect on the loss measurement in L-mode plasmas and is not included in the simulations. However, in rapidly rotating H-mode plasmas, it might have a bigger effect and should be investigated.

As an extension of the LIBP technique, it is pointed out that instead of using particle diagnostics that physically collect the lost fast ions, other approaches are possible. For example, IR camera measurements can be used as the detection system for the LIBP technique. In this application, the IR camera views modulated temperature excursions produced by promptly lost particles as they strike the vessel wall.[25] Another alternative detection approach is to design an experiment in which the first orbits pass through sightlines of a fast ion spectroscopy diagnostic, from which measurements of Doppler-shifted fast ion Dα (FIDA)[26] light are collected. For a constant edge neutral source, modulations in FIDA light are analogous to modulations in the prompt loss flux observed by FILD. Further, since the FIDA signal is proportional to the convolution of fast ion density (n_{FI}) and neutral density ($n_{neutral}$), the fast ion density from the LIBP source beam can be calculated and the neutral density profile can be inferred from the FIDA spectra from multiple radial channels.[27]

ACKNOWLEDGMENTS

[1] A. Loarte *et al.*, Nucl. Fusion **54**, 033007 (2014).
[2] H. Zohm, Plasma Phys. Control. Fusion **38**, 105 (1996).
[3] S. E. Sharapov *et al.*, Nucl. Fusion **53**, 104022 (2013).
[4] P. M. Schoch, A. Carnevali, K. A. Conner, T. P. Crowley, J. C. Forster, R. L. Hickok, J. F. Lewis, J. G. Schatz, Jr., and G. A. Hallock, Rev. Sci. Instrum. **59**, 1646 (1988).
[5] X. Chen, J. Hillesheim, P. M. Schoch, D. R. Demers, K. A. Connor, and D. Anderson, "HIBP designs for measurement of the electric field in HSX," http://meetings.aps.org/Meeting/DPP06/Session/BP1.56.
[6] R. E. Chrien, R. Kaita, and J. D. Strachan, Nucl. Fusion **23**, 1399 (1983).
[7] W. W. Heidbrink, "Tokamak diagnostics using fusion products," Ph.D dissertation (Princeton University, 1984).
[8] S. J. Zweben, Nucl. Fusion **29**, 825 (1989).
[9] S. Baeumel *et al.*, Rev. Sci. Instrum. **75**, 3563 (2004).
[10] M. García-Muñoz, H.-U. Fahrbach, H. Zohm, and the ASDEX Upgrade Team, Rev. Sci. Instrum. **80**, 053503 (2009).
[11] D. S. Darrow *et al.*, Rev. Sci. Instrum. **79**, 023502 (2008).
[12] X. Chen, R. K. Fisher, D. C. Pace, M. García-Muñoz, J. A. Chavez, W. W. Heidbrink, and M. A. Van Zeeland, Rev. Sci. Instrum. **83**, 10D707 (2012).
[13] D. C. Pace *et al.*, Rev. Sci. Instrum. **83**, 073501 (2012).
[14] D. Jiménez-Rey *et al.*, Rev. Sci. Instrum. **79**, 093511 (2008).
[15] M. Nishiura, M. Isobe, T. Saida, M. Sasao, and D. S. Darrow, Rev. Sci. Instrum. **75**, 3646 (2004).
[16] J. Kim, J. Y. Kim, S. W. Yoon, M. García-Muñoz, M. Isobe, and W. C. Kim, Rev. Sci. Instrum. **83**, 10D305 (2012).
[17] X. Chen, W. W. Heidbrink, G. J. Kramer, M. A. Van Zeeland, M. E. Austin, R. Nazikian, D. C. Pace, and C. C. Petty, Nucl. Fusion **53**, 123019 (2013).
[18] K. Shinohara *et al.*, Nucl. Fusion **51**, 063028 (2011).
[19] M. A. Van Zeeland *et al.*, Plasma Phys. Control. Fusion **56**, 015009 (2014).
[20] N. M. Ferraro, Phys. Plasma **19**, 056105 (2012).
[21] X. Chen, M. E. Austin, R. K. Fisher, W. W. Heidbrink, G. J. Kramer, R. Nazikian, D. C. Pace, C. C. Petty, and M. A. Van Zeeland, Phys. Rev. Lett. **110**, 065004 (2013).
[22] X. Chen, G. J. Kramer, W. W. Heidbrink, R. K. Fisher, D. C. Pace, C. C. Petty, M. Podesta, and M. A. Van Zeeland, Nucl. Fusion **54**, 083005 (2014).
[23] G. J. Kramer, R. V. Budny, A. Bortolon, E. D. Fredrickson, G. Y. Fu, W. W. Heidbrink, R. Nazikian, E. Valeo, and M. A. Van Zeeland, Plasma Phys. Control. Fusion **55**, 025013 (2013).
[24] C. Z. Cheng, Phys. Rep. **211**, 1 (1992).
[25] C. J. Lasnier, S. L. Allen, R. E. Ellis, M. E. Fenstermacher, A. G. McLean, W. H. Meyer, K. Morris, L. G. Seppala, K. Crabtree, and M. A. Van Zeeland, "Wide-angle ITER-prototype tangential IR and visible viewing system for DIII-D," Rev. Sci. Instrum. (these proceedings).
[26] W. W. Heidbrink, Rev. Sci. Instrum. **81**, 10D727 (2010).
[27] N. G. Bolte, "Measurements and modeling of fast-ion light from edge neutrals in the DIII-D tokamak," Ph.D dissertation (University of California, Irvine) (unpublished).